



Effects of latent heat storage and controls on stability and performance of a solar assisted heat pump system for domestic hot water production



W. Youssef, Y.T. Ge^{*}, S.A. Tassou

RCUK National Centre for Sustainable Energy Use in Food Chains (CSEF), Institute of Energy Future, Brunel University London, Uxbridge, Middlesex UB8 3PH, UK

ARTICLE INFO

Article history:

Received 22 February 2017

Received in revised form 25 April 2017

Accepted 26 April 2017

Keywords:

Solar assisted heat pump

Domestic hot water production

PCM heat exchanger

Experimental investigation and controls

ABSTRACT

Solar assisted heat pump systems have been widely applied in domestic hot water productions due to their sustainability and stability in operations. However, their performance efficiency requires further improvement using advanced technologies such as energy storage with phase change materials (PCM) and optimal system controls. Accordingly, a test rig of a new indirect solar assisted heat pump (IDX-SAHP) system has been designed, built and instrumented. The IDX-SAHP system consists of three operational loops: solar thermal, solar assisted heat pump and load profile. A PCM heat exchanger tank was purposely designed and installed in the system solar thermal loop to store solar energy, when applicable, and release heat when required by the heat pump. In addition, an air cooling heat exchanger was also installed in the solar thermal loop to absorb heat from the ambient air for the heat pump. A detailed control strategy has been designed and implemented for the system for efficient operation in different modes and maintain constant load supply water temperature during an operational day. In different weather conditions of sunny and overcast, comprehensive measurements were carried out on the test rig and system structures with and without the PCM tank. Test results showed that the system could efficiently meet the daily domestic hot water demand and the PCM heat exchanger integration exerted a significant effect on system stability and performance efficiency. Quantitatively, the average COP of the IDX-SHAP system with a PCM tank could increase 6.1% and 14.0% on sunny and cloudy days respectively compared to systems without PCM tank integration.

© 2017 Elsevier Ltd. All rights reserved.

1. Introduction

In the UK, up to 50% of national energy is consumed for heating purposes by direct burning of fossil fuels, in particular natural gas (IEA, 2007). The extensive consumption of fossil fuels or natural gas has caused significant atmospheric pollution, global warming, rising energy costs and threatens future energy shortage. In such circumstances, meeting CO₂ emission reduction targets remain a challenge for the country if alternative energy resources or technologies cannot be applied for heating. The heating demand can be met by green technologies and advanced systems such as a solar thermal, air-water heat pump, geothermal heat pump and their integrations. Solar domestic water heaters (SDWHs) have been increasing in popularity in the UK and other countries worldwide and can greatly save energy for water heating in the summer (Freeman, 1997). However, the large temperature difference between the solar collector and ambient temperatures during winter has greatly reduced system performance such that assistant

heaters such as gas, wood boilers or electric heaters must be added (Weiss, 2003; Ayome et al., 2011). The air source heat pump water heaters are compact, simpler and economic but also work less efficiently over the cold winter period (Aguilar et al., 2005). These situations may be improved with the integration of geothermal heat sources, as heat is being drawn from the warmer earth in winter. However, the high capital costs and property alterations expected for these geothermal heat pumps make them less attractive for existing homes (Aguilar et al., 2005). Of these alternative substitutes, a Solar Assisted Heat Pump (SAHP) system has been deemed the more feasible option when taking into consideration important factors such as cost, application area limitation and constant water heating production etc. (Eicher et al., 2012).

The combination of solar energy and heat pump technology can be classified into two categories: direct expansion solar assisted heat pump (DX-SAHP) and indirect expansion solar assisted heat pump (IDX-SAHP) (Chen and Yu, 2017). For a DX-SAHP system, the solar collector also acts as the evaporator of the heat pump unit, thereby making the system more compact but requiring greater heat pump working fluid charge (Facão and Carvalho, 2014). In addition, when there is insufficient solar radiation, the

^{*} Corresponding author.

E-mail address: Yunting.Ge@brunel.ac.uk (Y.T. Ge).

Nomenclature

<i>AWHX</i>	air-water heat exchanger	<i>TEV</i>	thermostatic expansion valve
<i>BMS</i>	building management system	ΔT	temperature difference (K)
<i>C_p</i>	specific heat capacity (J kg ⁻¹ K ⁻¹)	<i>W</i>	work input (W)
<i>COP</i>	coefficient of performance	<i>WFC</i>	water fan cooler
<i>DHW</i>	domestic hot water	<i>WST</i>	water storage tank
<i>DX</i>	direct		
<i>h</i>	enthalpy (J kg ⁻¹)	<i>Subscripts</i>	
<i>IDX</i>	indirect	<i>Comp</i>	compressor
<i>m</i>	mass flow rate (kg s ⁻¹)	<i>H</i>	heating
<i>PCM</i>	phase change material	<i>Ref</i>	refrigerant
<i>Q</i>	heat transfer rate (W)	<i>Sys</i>	system
<i>SAHP</i>	solar assisted heat pump	<i>W</i>	water
<i>T</i>	temperature (°C)		

solar collector/evaporator cannot absorb enough heat required by the heat pump and thus negatively affect system performance (Sun et al., 2015). On the other hand, with an IDX-SAHP system, solar radiation transfers heat to water flow through the solar collector and then provides heat to the heat pump evaporator. In such circumstances, the working fluid charge in the heat pump can be greatly reduced. The IDX-SAHP can also be further classified into three design layouts based on different heat source arrangements: series, parallel and dual source (Kamel and Fung, 2014). For a series IDX-SAHP system, the solar energy is collected by a solar collector and stored in a water storage tank which is used as the only heat source for the heat pump. Solar heat sources may be insufficient for meeting building heating demands in certain weather conditions and time periods. A SAHP system used for mushroom drying was experimented which was relatively similar to the series IDX-SAHP scheme for space heating (Şevik et al., 2013). The COP of the system fluctuated between 2.1 and 3.1 and the study demonstrated that heat pump performances greatly improve with the addition of solar energy. In addition, a series IDX-SAHP system used for space heating in Turkey was experimented (Bakirci and Yuksel, 2011). When solar gain was available, the solar energy was first stored in a storage tank and then passed to the heat pump evaporator through a heat exchanger installed inside the tank. In cloudy or night mode, the energy was extracted directly from the storage tank to the evaporator. The average COP of this system was 2.9. However, research outcomes showed that improvements in system performance were limited by storage tank designs and configurations.

For a parallel IDX-SAHP system, a conventional solar system operates in parallel with an air source heat pump such that the heat pump operation is independent of solar energy availability. Therefore, the building heating load can be met by either the solar energy or air source heat pump. A parallel SAHP system was simulated and compared the system performances with both ground and air source heat pumps (Carbonell et al., 2014). The ground source heat pump appeared promising in terms of absolute electricity saving when paralleled with solar energy. For any of the applicable heat pump systems, CO₂ working fluid is a feasible option considering its environmentally friendly behaviours, superb thermophysical properties and system compactness etc. (Deng et al., 2011).

For a dual source IDX-SAHP system, two heat pump evaporators are installed and utilised with different heat sources. One is installed inside the solar storage tank to collect solar energy and the other outside the building to absorb heat from ambient air.

One evaporator will be controlled to operate within the system if it produces a higher COP. A multifunctional IDX-SAHP system has been simulated and experimentally validated which could supply space heating, cooling and domestic hot water (DHW) by switching different operating modes on/off as required (Wang et al., 2011). The heating mode was implemented in a dual source system while the space cooling was achieved via a liquid to the air heat exchanger installed indoor. It was recommended that system performance could be further enhanced over the winter in areas where higher solar irradiances were available. A feasibility analysis of a dual tank IDX-SAHP system was conducted and compared with a traditional thermal solar system using numerical simulation (Sterling and Collins, 2012). The analysis outcomes also verified that dual tank was the most efficient configuration of the IDX-SAHP systems and the greatest potential to be applied into a SAHP system for DHW. This led to an experimental investigation of multi-configuration SAHPs (Banister et al., 2014a, 2014b), which could be used to validate the numerical methods and control strategy to be developed and reliability of the systems. The study was effective in identifying the modes of operation and further numerical validation with focus on thermal storage stratification (Banister et al., 2014a, 2014b).

Of these IDX-SAHP systems, the parallel and dual source are preferable in terms of system operational stability. However, the solar storage tank performance, control strategy, system efficiency and component compactness need to be further improved. For a conventional solar water storage tank, stratification remains a big issue, with an impact extending to system controls, theoretical analyses and overall system performance. Alternatively, a phase change material (PCM) such as organic paraffin wax may be a better substitute for use in the solar energy storage tank when considering its thermal stability and resulting tank compactness, although further verification is needed (Sharif et al., 2015; Farid et al., 2004).

In this paper, a new IDX-SAHP test system was designed, installed and instrumented. A PCM storage heat exchanger tank and an air-source heat exchanger were purposely built and installed in the system solar thermal loop and connected to the heat pump evaporator. Subsequently, the heat source from either solar energy or ambient air can be applied for the heat pump. In addition, a control strategy for the system was purposely designed and implemented so as to determine the optimal operation of the IDX-SAHP system. Comprehensive experimental investigations were carried out in the test rig to evaluate and compare system operation and performance in different weather conditions and

structures with and without PCM tank installations. The research outcomes can lead to the optimisation of future system designs and controls.

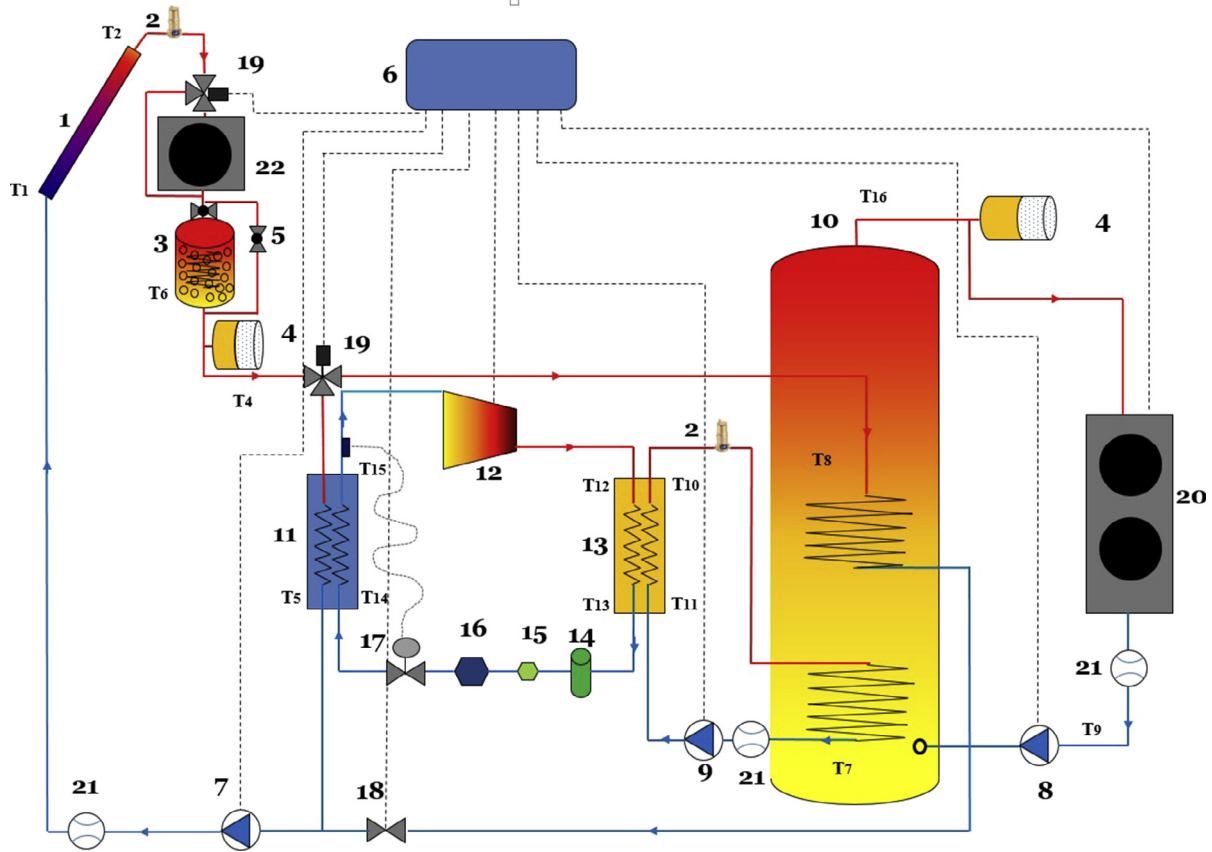
2. Test facility

2.1. Test rig description

The test rig of an IDX-SAHP system is shown schematically in Fig. 1. The system was designed to be installed for a standard UK dwelling to cover up to 350 L per day of domestic hot water (DHW). The test system consists of a number of main components which are numbered in Fig. 1. The evacuated tube collector was installed outdoor on a building roof and it has a total surface area of 3.021 m² and 52° tilt angle with south facing orientation. The insulated water storage tank (WST) has a capacity of 300 L and is made of stainless steel with two coils immersed inside: one for direct solar thermal operation and the other for the IDX-SAHP

system. There is also a phase change material (PCM) heat exchanger tank installed to store excessive solar energy during day-time operation. The PCM (Organic PCM, Paraffin) has a melting point of 17 °C with a mass of 30 kg charged in the heat exchanger tank. The energy stored in the tank is designated to be used as heat source for the heat pump during the night or when the solar irradiance during the day is poor. The heat pump uses R134a as refrigerant and consists of typical components and accessories such as a compressor, liquid-cooling plate evaporator, liquid-cooled plate condenser, thermostatic expansion valve (TEV), filter, receiver, and sight glass etc. To clearly demonstrate the test rig and the PCM heat exchanger tank in the system, their photos are shown in Fig. 2 in which some main components in the test rig and detailed PCM structures are indicated.

The solar collector operates periodically between two loops. The first one is a direct solar thermal loop which is applied to produce hot water completely from solar energy through the solar collector and transport the hot water to the WST, similar to any traditional



- | | | | |
|----|--------------------------|----|------------------------------|
| 1 | Evacuated tube collector | 12 | Compressor |
| 2 | Deaerator | 13 | Condenser |
| 3 | PCM heat exchanger tank | 14 | Receiver |
| 4 | Expansion tank | 15 | Filter |
| 5 | Bypass- ball valve | 16 | Sight glass |
| 6 | BMS controller | 17 | Thermostatic expansion valve |
| 7 | Solar / heat source pump | 18 | 2-way valve |
| 8 | Load simulation pump | 19 | 3-ways valve |
| 9 | Heat sink pump | 20 | Fan cooler |
| 10 | Water storage tank | 21 | Flowmeter |
| 11 | Evaporator | 22 | Air-water heat exchanger |

Fig. 1. Test rig layout.

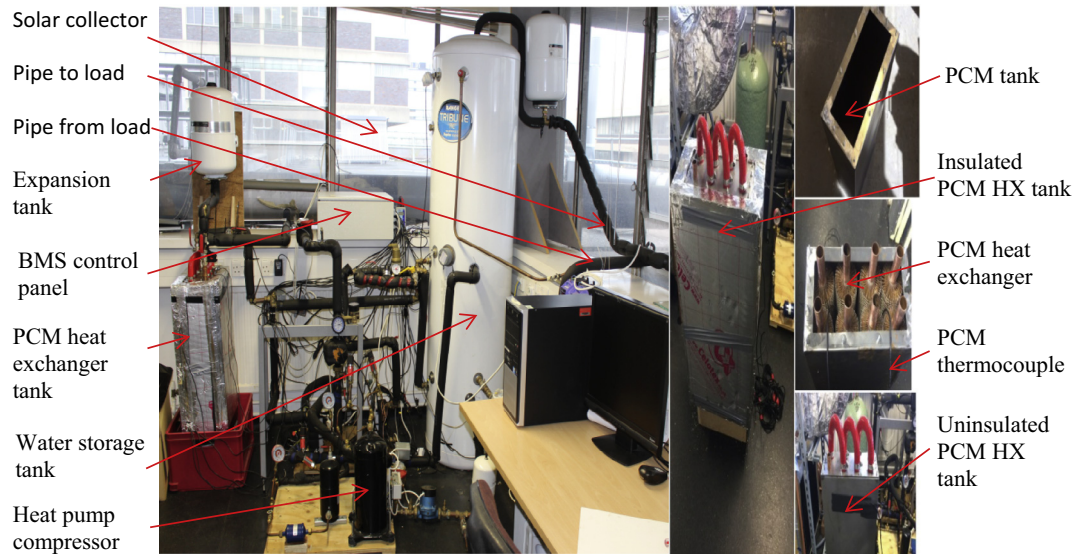


Fig. 2. PCM tank design and test rig setup.

solar thermal system. This loop will work independently if the solar irradiance is sufficient to heat up the WST. In the second loop, the solar collector operates as a heat source for the IDX-SAHP. This applies when the solar irradiance is not sufficient to heat up the WST directly but it is enough to act as a heat source to the heat pump through the liquid-cooling evaporator and/or to charge the PCM tank when the heat pump is not switched on. In the case of insufficient solar irradiance or deficient energy stored in the PCM tank, heat source from ambient air through an air-water heat exchanger (AWHX) will be applied for the heat pump. The designed capacity of the AWHX is 10 kW and the power consumption of its electric fan is 0.5 kW. To ensure successful operation, the AWHX is installed at the supply water pipe of the solar collector just prior to the PCM heat exchanger tank. For the IDX-SAHP system, the WST is heated up through its internal bottom coil which is connected to the liquid-cooled condenser of the IDX-SAHP. The operations of these two loops are controlled automatically by two motorised valves which are described in Section 2.3. The heat transfer liquid used in either evaporator, condenser or the solar thermal loop is a mixture of 30% Ethylene Glycol and 70% water with a freezing temperature of $-15\text{ }^{\circ}\text{C}$.

There is also an addition loop called load simulation loop which includes an expansion tank, a water fan cooler (WFC) and a water pump connected to WST. Since it is hard to implement the experiment in an actual dwelling, the load simulation loop has been purposely constructed in order to simulate and establish a standard UK dwelling hot water consumption profile during a long typical day (EST, 2008). Based on the designed load profile, the circulation pump speed is controlled accordingly by an inverter in order to modulate the required feed water flow rate to the storage tank. This can be implemented by controlling the pump motor frequency as it is directly proportional to the water flow rate. In the meantime, as shown in Fig. 1, the feed water temperature at the WFC outlet is controlled by the water cooler's fan speed and is maintained as low as ambient air temperature. One of novelties of this study is that a fully automated control strategy by building management system (BMS) was deployed in order to maintain the outlet WST temperature at $55\text{ }^{\circ}\text{C}$ by controlling consequently with each operational mode. This can contribute significantly to facilitate further development and actual system application.

To measure extensively the performance of the system and its main components, a number of temperature sensors from T1 to

T16 indicated in Fig. 1 were installed in the system. A thermocouple T6 was inserted and installed in the middle of the PCM tank to measure the PCM temperature T_{pcm} . In addition, two pressure transducers were installed respectively at the inlet and outlet of the heat pump compressor. The measurements also included the water flow rates of solar thermal loop after pump 7 and heat pump condenser water loop after pump 9, and the power consumptions of compressor, AWHX fan and water pumps 7 and 9. The detailed specifications and accuracies of the main measurement instruments used in the system are listed in Table 1.

2.2. Test rig operation modes

In order to increase the system efficiency, the system should utilise the solar energy as much as possible corresponding to the DHW load demand and weather condition. The operation modes can be classified as below:

Solar and PCM Charging Modes: In these two modes, the system works as a conventional solar thermal system to cover the DHW load demand and simultaneously charge the PCM tank when applicable. These two modes operate in the same loop which has the following sequence:

Solar collector \rightarrow V19 (after the solar collector, left port open and down port closed to bypass the AWHX) \rightarrow PCM tank \rightarrow expansion tank \rightarrow V19 (after the PCM tank, right port open and down port closed) \rightarrow WST middle immersed coil \rightarrow V18 (open) \rightarrow pump 7 (on) \rightarrow flowmeter \rightarrow solar collector.

IDX-SAHP Mode: In this mode, the heat pump will take responsibility to meet the DHW load demand. It consists of three related circulation loops: condenser, heat pump and evaporator loops. In the condenser loop, the glycol water is the heat transfer fluid circulating around the heat pump condenser water side and the bottom

Table 1
Main measurement instruments used in the experimental system.

Parameters	Type	Range	Accuracy
Temperatures	Thermistor 10 K	-55 to $125\text{ }^{\circ}\text{C}$	$\pm 0.1\text{ }^{\circ}\text{C}$
Pressures	Pressure Transmitter	-1 to 34 bar	$\pm 0.3\%$
Flowmeter	Pulsed Screwed Water Meter	35 – 7000 L/h	$\pm 5\%$
Solar irradiance	Pyranometer	0 – 2000 W/m^2	$\pm 10\text{ W/m}^2$
Power meter	Power Quality Analyser	0 – 20 MW	$\pm 1\%$

immersed coil of the WST. The circulation of this loop operates in the following sequence:

Pump 9 → condenser (water side) → WST bottom immersed coil → flowmeter → pump 9.

In the heat pump loop, the heat is extracted from the heat source and delivered to the heat sink via a vapour compression heat pump cycle. The refrigerant in the cycle circulates in the following sequence:

Compressor → condenser (refrigerant side) → receiver → sight glass → filter → TEV → evaporator (refrigerant side) → compressor.

In the evaporator loop, one of the following applicable loop circulations can be selected and controlled based on relevant heat source utilisation:

- (1) AWHX is off- this operation will be enabled if there is enough heat source from solar energy of either solar irradiance or the PCM tank. The circulation of this loop operates in the following sequence:

Solar collector → V19 (after the solar collector, left port open and down port closed to bypass the AWHX) → PCM tank → expansion tank → V19 (after the PCM tank, right port closed and down port open towards the evaporator) → evaporator (water side) → pump 7 → flowmeter → solar collector.

- (2) AWHX is switched on-this operation will be enabled if there is no enough heat source from either solar irradiance or the PCM tank. The circulation of this loop operates in the following sequence:

Solar collector → V19 (after solar collector, left port closed and down port open towards the AWHX) → air-water heat exchanger (AWHX) → PCM tank → expansion tank → V19 (after PCM tank, right port closed and down port open towards the evaporator) → evaporator (water side) → pump 7 → flowmeter → solar collector.

It should be noted that in Fig. 1 two bypass- ball valves 5 were installed respectively at the inlet and by-pass pipes of the PCM tank. These two valves are utilised and controlled to measure and compare the performance of system with and without PCM tank integrated.

2.3. System control strategy

As shown in Fig. 3, the system control strategy has been purposely designed to maintain the water temperature at the middle of the WST (T8) at 55 °C with ±2 K dead band during a 24-hour operational day. If the T8 is less than its permitted lower value (53 °C), the control will check the instant solar irradiance G and the supply water temperature (T4) to the WST. If there is no enough solar irradiance ($G < 500 \text{ W/m}^2$) and the T4 is less than

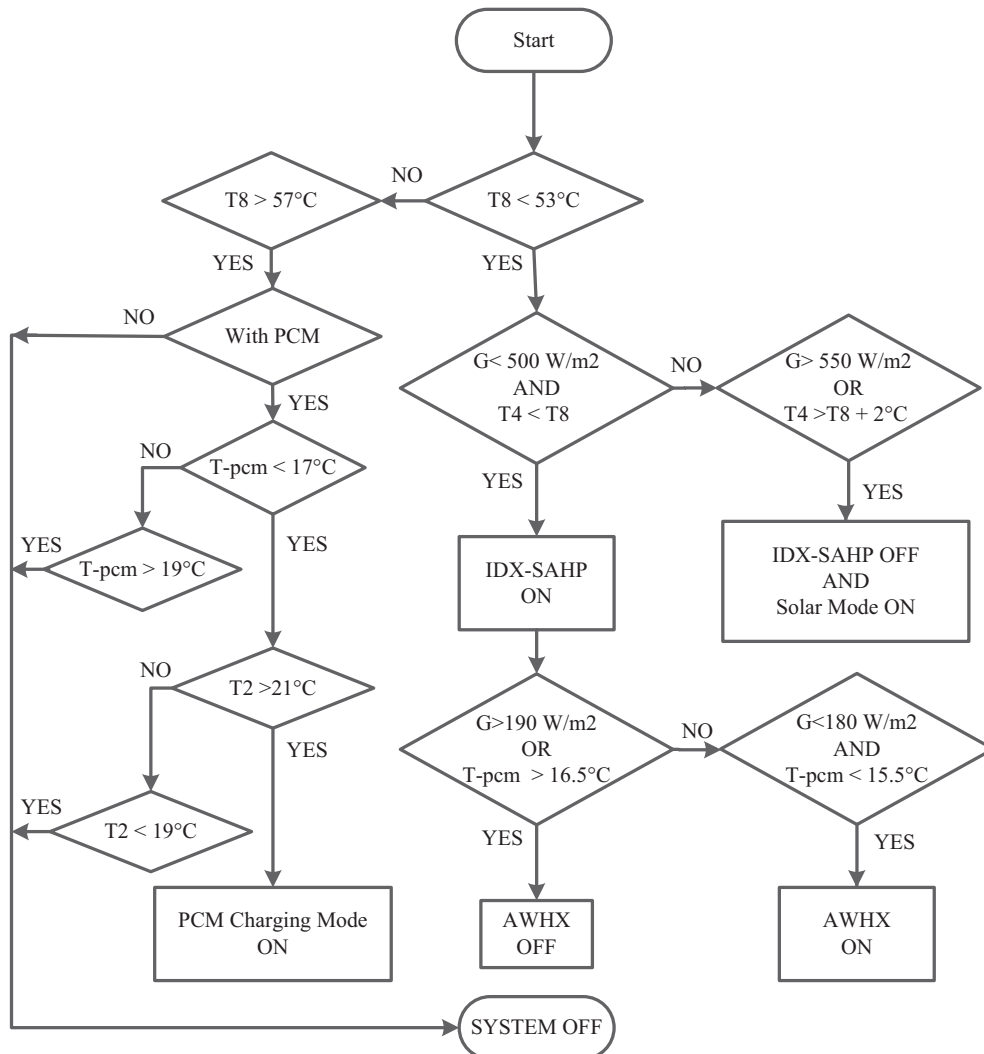


Fig. 3. Flow chart of system control strategy.

T8, the IDX-SAHP should be switched on. The control will then check the applicable heat source for the IDX-SAHP. If G is greater than 190 W/m^2 or PCM tank temperature T_{pcm} is larger than $16.5 \text{ }^\circ\text{C}$, either the solar irradiance or heat stored in the PCM tank can be used as the heat source such that the AWHX should be turned off. Otherwise, the AWHX needs to be switched on considering of a specific dead band for each parameter so that the ambient air can be utilised as the heat source. On the other hand, if the solar irradiance is sufficient ($G > 550 \text{ W/m}^2$) or T_4 is greater than T_8 plus 2 K dead band, the IDX-SAHP should be off and the solar mode will be on. When the T_8 is controlled within the setting point band ($55 \pm 2 \text{ }^\circ\text{C}$), the system maintains its operating state. If T_8 is above its higher band, the control will switch off the whole system if the PCM tank is not applied. Otherwise, it needs to determine if the PCM tank needs to be charged by assessing the PCM tank temperature (T_{pcm}) and water temperature at the solar collector outlet (T_2). If the T_{pcm} is less than $17 \text{ }^\circ\text{C}$, the PCM charging mode needs to be turned on when T_2 is greater than $21 \text{ }^\circ\text{C}$, otherwise, the whole system will be off (2 K dead band for T_2). Alternatively, if the T_{pcm} is greater than $17 \text{ }^\circ\text{C}$ and less than $19 \text{ }^\circ\text{C}$, nothing will be changed. However, if the T_{pcm} is higher than $19 \text{ }^\circ\text{C}$, the whole system will be off.

2.4. Experimental procedure

In order to examine experimentally the effect of the PCM tank on system stability and performance, four test days have been conducted in 24 hours each at four combined climate conditions and PCM integrations. These included sunny with and without PCM tank and cloudy with and without PCM tank. As shown in Fig. 4, the solar irradiances during two sunny test days with and without

PCM tank were almost steady with maximum values of 621 W/m^2 and 625 W/m^2 respectively while the irradiances during those two cloudy test days had too many fluctuations. It is also noticed that the solar energy was only available during day time when the solar irradiance was greater than zero. Figs. 5 and 6 show the variations of ambient and WST load feed water (T_9) temperatures during all these four test days. It should be noted that all temperature, power, irradiance and pressure logging data were based on five minutes interval whereas any other logging data was based on the change of each sensed value. As explained earlier, the feed water supply to the WST is mainly from domestic tap water. Therefore, the minimum temperature it could achieve was the same as the ambient temperature due to the heat transfer limitation of the WFC. Fig. 7 shows the feed water flow rate or load profile supplied to the WST for each operational day. Each flow rate was controlled by a variable circulation pump speed which was regulated by BMS according to the specified load profile (EST, 2008). It is seen that the load profile for each test day was controlled almost the same with each other which of course should be independent on weather conditions and system designs.

2.5. Thermodynamic analysis

The mass flow rate of refrigerant is calculated by the energy balance of water and refrigerant sides across the condenser assuming there is no heat loss to ambient:

$$\dot{m}_{\text{ref}}(\Delta h)_{\text{ref}} = \dot{m}_w C_{p,w}(\Delta T)_w \tag{1}$$

The thermo-physical properties of R134a used for thermodynamic analysis are calculated using Engineering Equation Solver (EES®) (Klein, 2014).

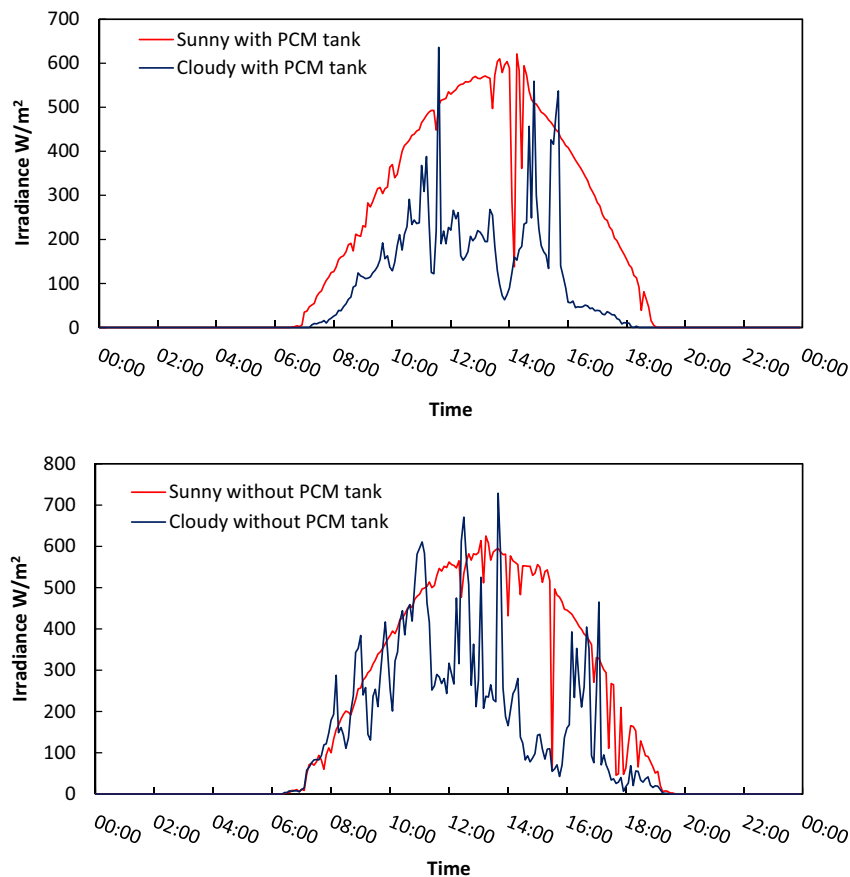


Fig. 4. Variations of solar irradiances during four test days.

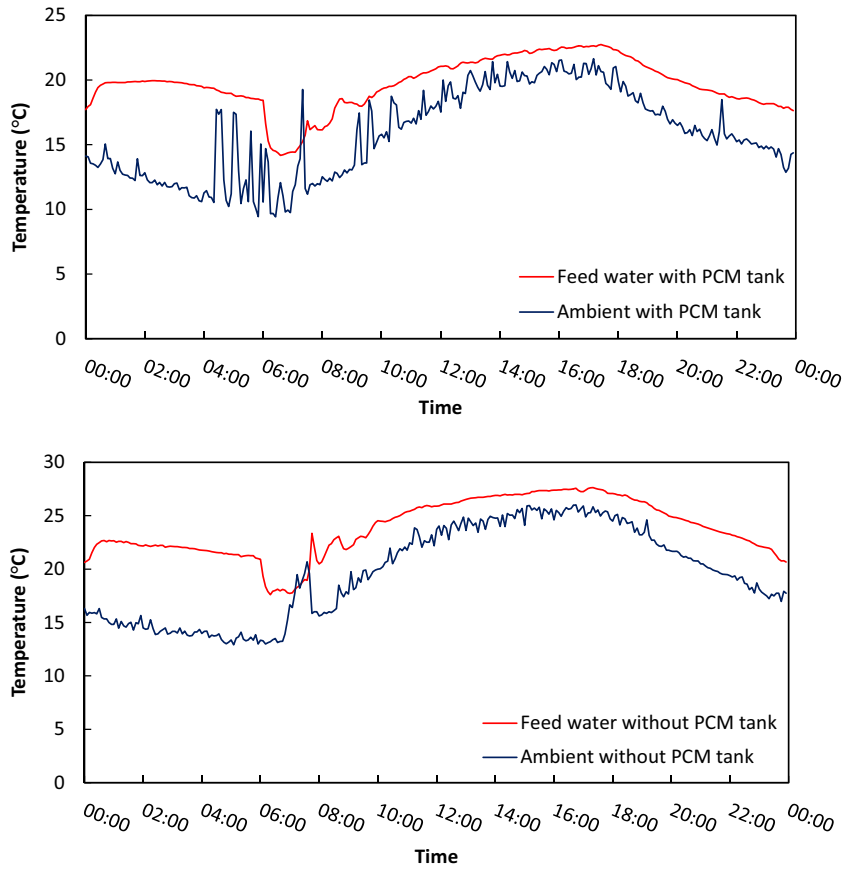


Fig. 5. Variations of ambient and feed water temperatures during two sunny test days.

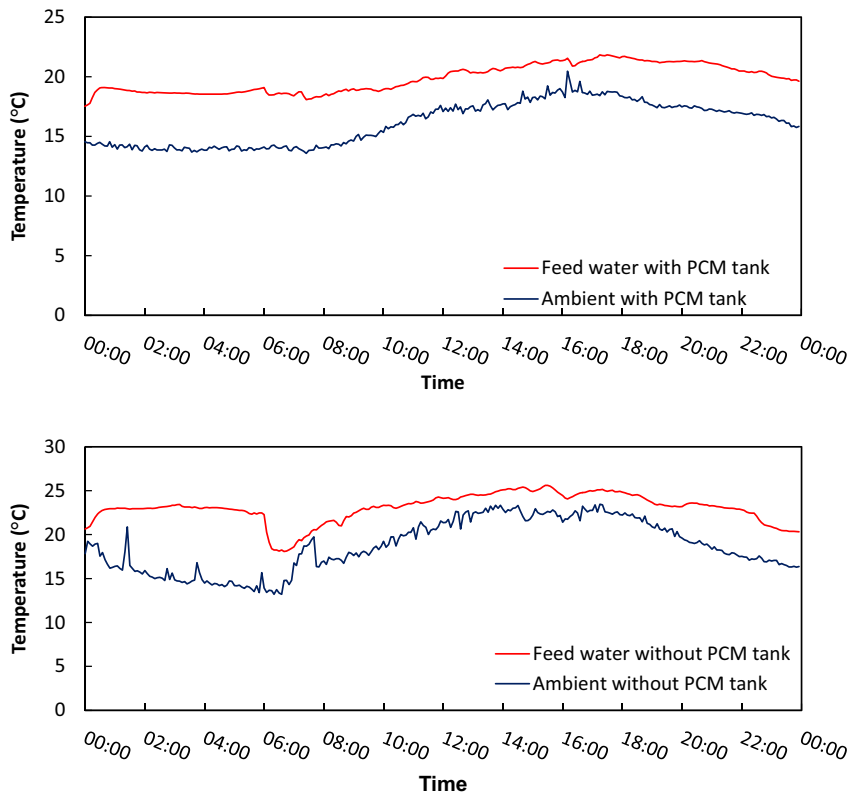


Fig. 6. Variations of ambient and feed water temperatures during two cloudy test days.

The heating capacity of the system in IDX-SAHP mode is calculated based on water side inlet and outlet parameters of the condenser:

$$Q_h = \dot{m}_w C_{p,w} (\Delta T)_w \tag{2}$$

The heating COP of the system is calculated with the ratio of the total heating capacity to the total power consumption of the system:

$$COP_{sys} = \frac{Q_h}{W_{comp} + W_{WFC} + W_{pumps}} \tag{3}$$

3. Experiment findings and discussions

Based on the proposed system control strategy described previously, experimental investigations were carried out on the IDX-

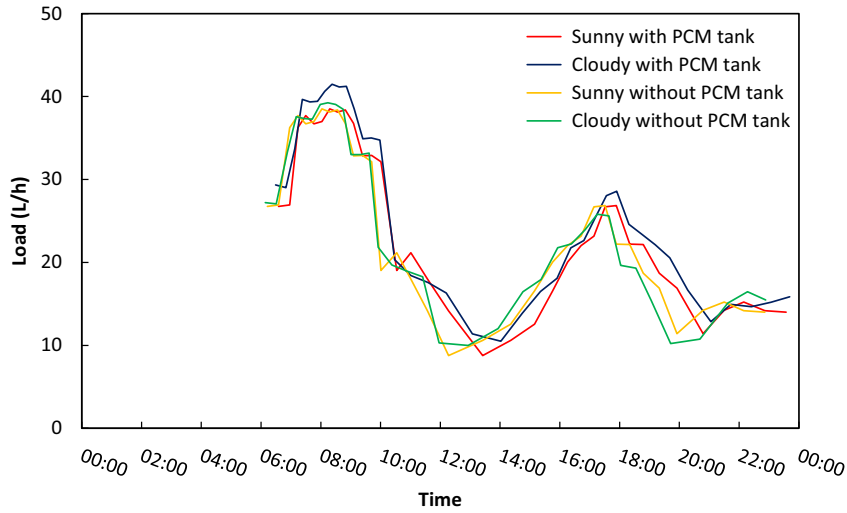


Fig. 7. Variations of load profiles during all four test days.

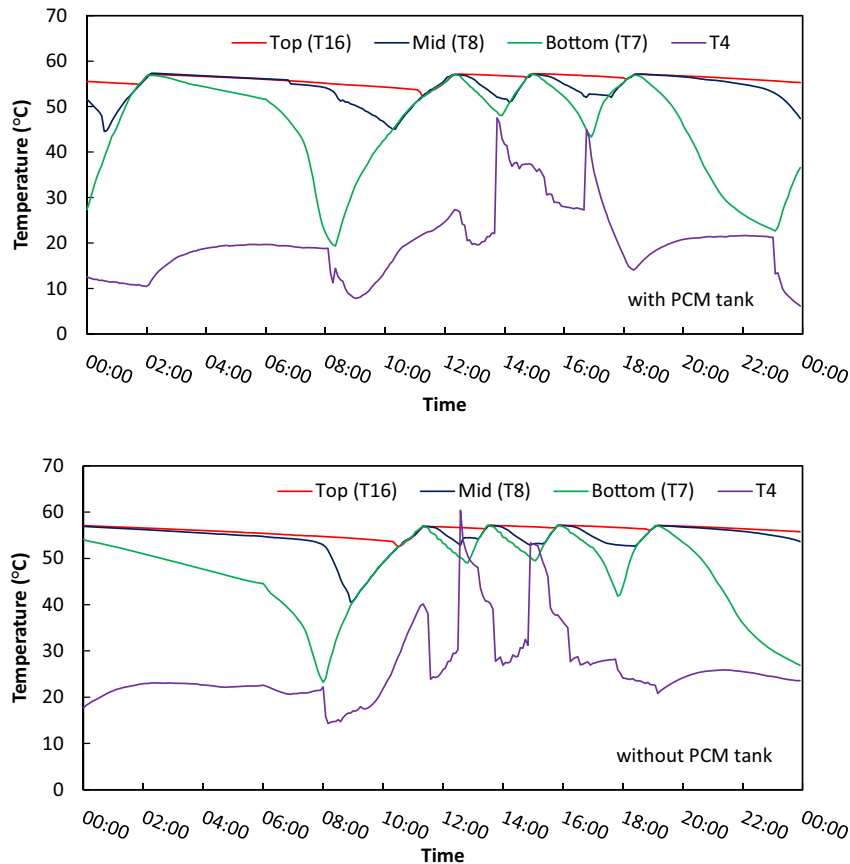


Fig. 8. Variations of WST water temperatures and temperature T4 during two sunny test days.

SAHP system during those four test days and some of the test results are demonstrated and evaluated in this section. As illustrated in Figs. 8 and 9 for the temperature development inside the WST, the system could meet the DHW demand by supplying hot water flow from the WST top with temperatures between 52 °C and 57 °C during all these four test days. To understand clearly the system controls, the variation of water temperature from the PCM tank outlet (T4) is also presented in each plot. As indicated in Fig. 3, the temperatures of T8 and T4 and solar irradiance will determine the operation of the IDX-SAHP. It is observed that for each test day around 8 am there was a big temperature drop at the tank bottom (T7) before the water temperature T8 dropped below the lower band of its setting point. This abrupt

decrease in the bottom tank water temperature T7 was due to the starting of DHW load demand in the morning on that day as shown in Fig. 7. Meanwhile, the feed water temperature for each operational day was different due to various ambient air temperatures. Consequently, there were different lowest bottom tank water temperatures for these four test days. To fully understand the system performance, the test results of these four operating days are explained separately in the following parts.

For the sunny test day with PCM tank, the compressor started at midnight with no heat stored in the PCM tank as the PCM temperature (T-PCM) inside the PCM tank was 14.5 °C, as shown in Fig. 10, which was below its melting point. That resulted in switching the AWHX on during that period to utilise the heating source from the

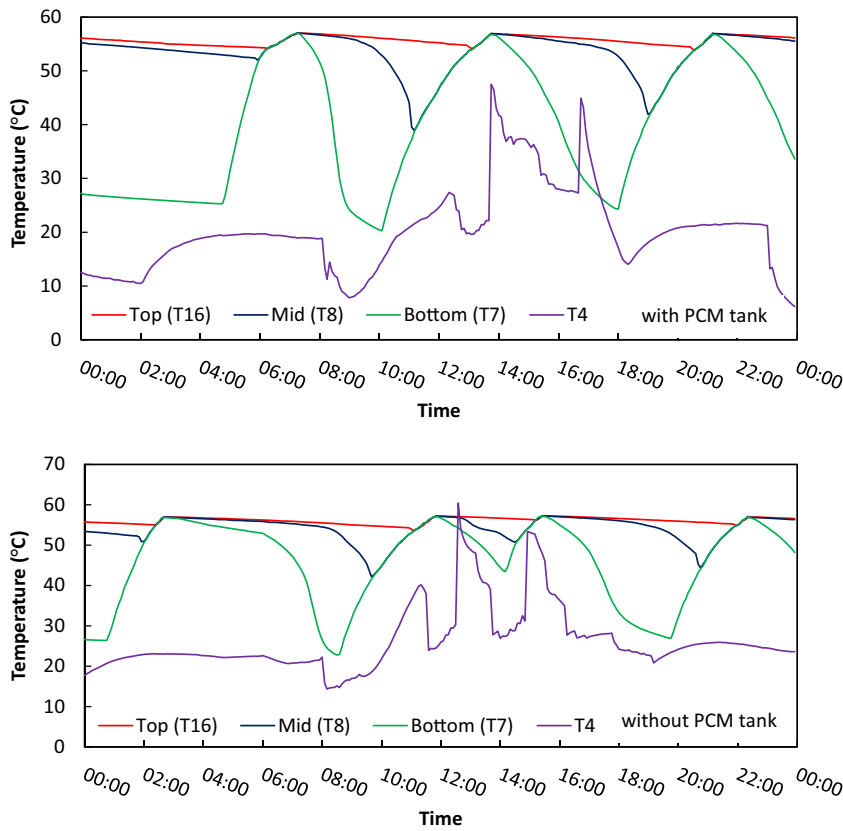


Fig. 9. Variations of WST water temperatures and temperature T4 during two cloudy test days.

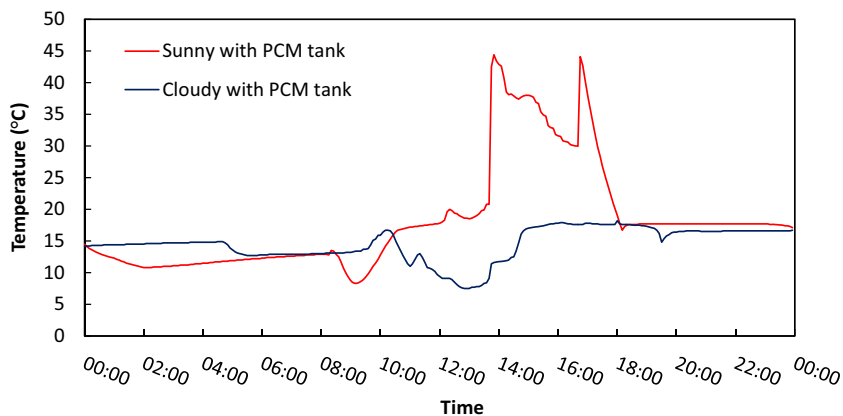


Fig. 10. Variations of PCM tank inside temperatures during two test days.

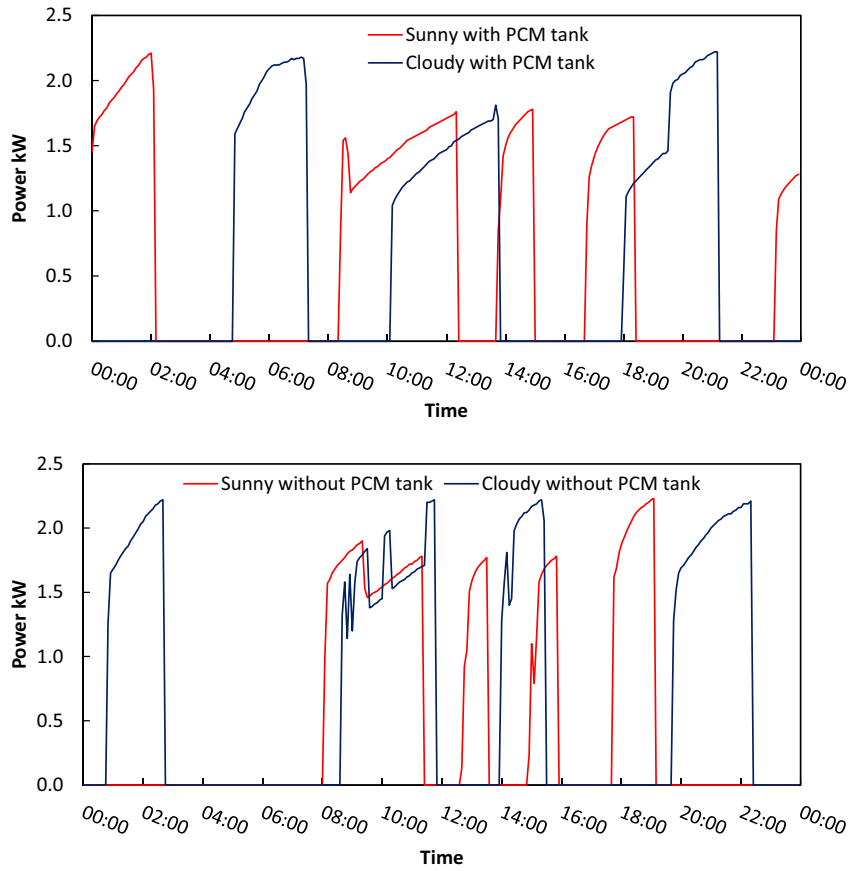


Fig. 11. Variations of system power consumptions during four test days.

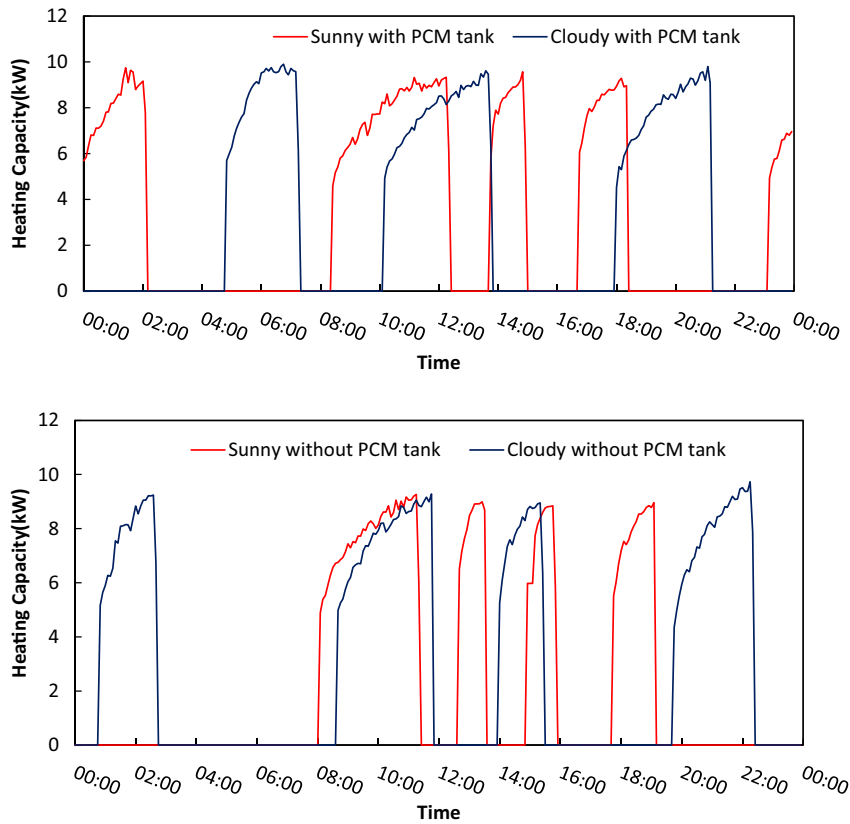


Fig. 12. Variations of system heating capacities during four test days.

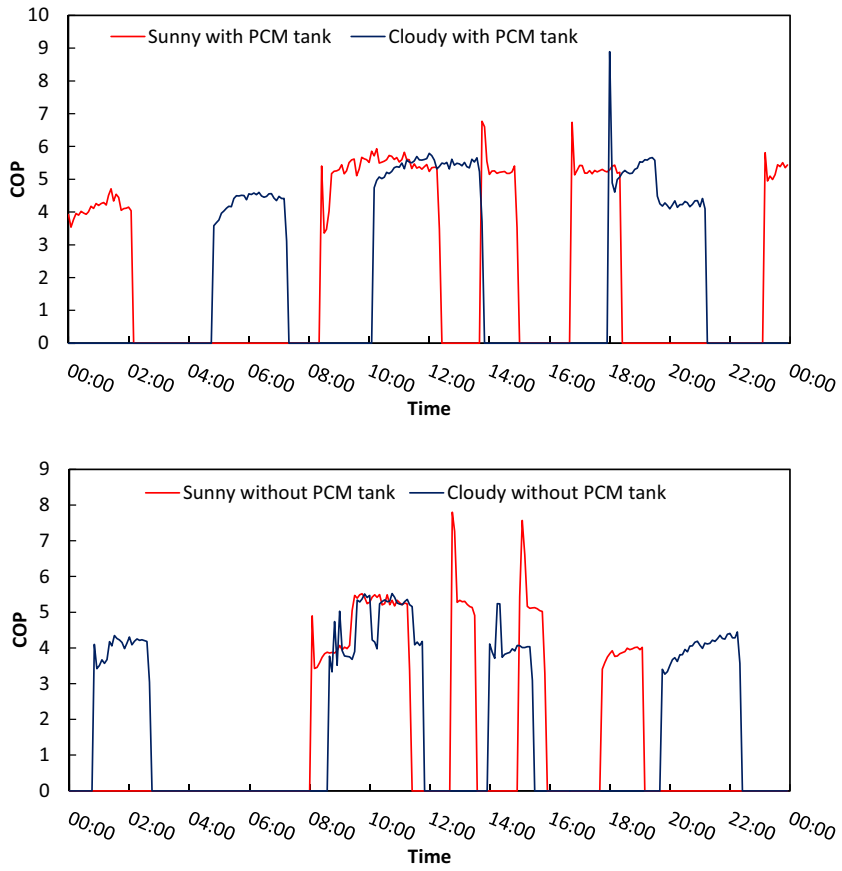


Fig. 13. Variations of system COPs during four test days.

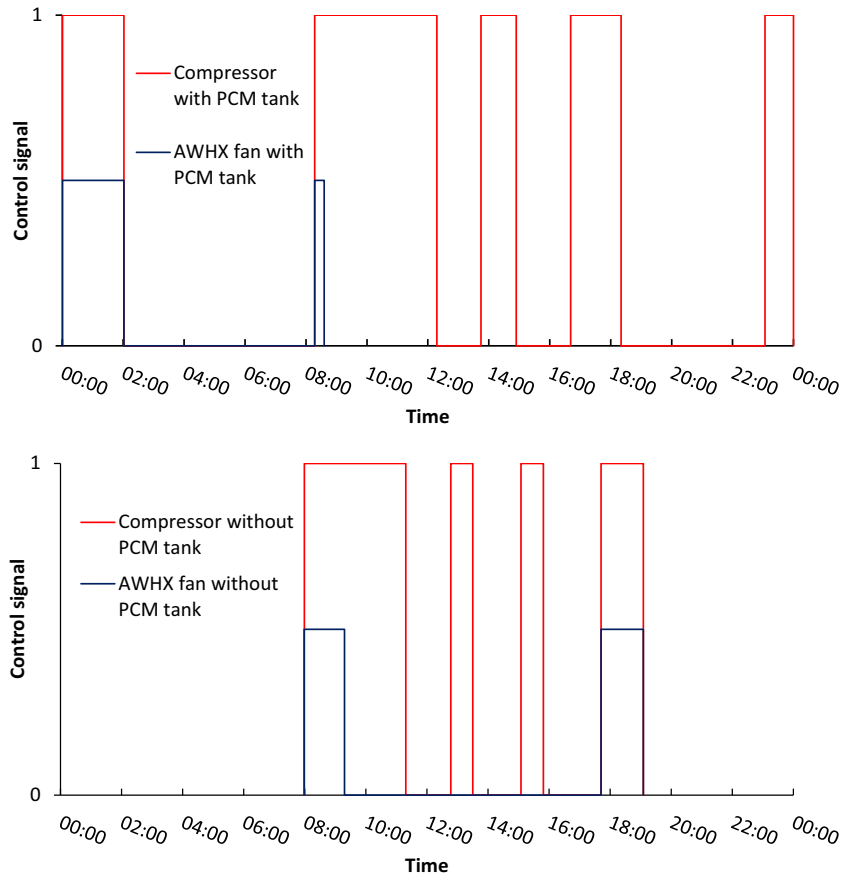


Fig. 14. Variations of compressor and AWHX fan control signals during two sunny test days.

ambient air, as shown later on in Fig. 14. The heat pump compressor operated until 2:05 pm when T8 was higher than 57.0 °C and the system then started in PCM charging mode. During this period the maximum value for the total power consumption, condenser capacity and COP were 2.2 kW, 9.632 kW and 4.7 respectively as shown in Figs. 11, 12 and 13 each. The PCM charging mode operated until 8:20 am when T8 started to drop below 53 °C and the heat pump compressor was switched on again. Up to that point, the PCM inside the tank was still not charged significantly since its temperature was only at 12.8 °C such that the AWHX needed to operate. The AWHX operated until at 8:35 am when the solar irradiance G reached above 190 W/m² and could be utilised as the heat source for the IDX-SAHP. Correspondingly, at that instant, the system power consumption thus dropped abruptly and the COP increased sharply, as shown in Figs. 11 and 13 respectively. After that the system power consumption and condenser heating capacity increased gradually but COP varied. The heat pump compressor kept running until at 12:20 when T8 started to be higher than 57 °C again. During this period, the PCM temperature T-pcm started to drop to its minimum temperature at 8.3 °C at 9:10 am since the AWHX was on at the beginning. The T-pcm was then picked up at different rates when the AWHX was off and more solar irradiances were available. These included significant 8.7 °C increase from 9:10 am to 10:50 am due to sensible PCM heating process and only 1 °C increase from 17 °C to 18 °C at the time period between 10:55 am and 12:05 because of latent PCM heating process involved. At 12:05, the PCM was totalled melted and from there only sensible PCM heating existed such that the T-pcm increased abruptly from 12:05 to 12:20. From there, the whole system was shut down since the T-pcm was higher than 19.0 °C. The tank water temperature at T8 thus started and continued to drop to

below 53.0 °C at 13:40 when either IDX-SAHP or solar mode needs to be controlled. From that time as shown in Fig. 8, although the solar irradiance G was higher than 500 W/m², the water temperature T4 was still lower than T8 such that the IDX-SAHP mode was on and the AWHX was off due to the higher G values. Meanwhile, the PCM temperature T-pcm had a big jump due to the high temperature from the solar collector outlet and the PCM sensible heating process. The T-pcm then followed the changes of the solar collector outlet water temperature and the PCM absorbed and released heat respectively to the water flow depending on the temperature differences between these two temperatures. Correspondingly, from 19:15 the water received heat from the heat stored in the PCM tank. The system was switched off at 14:55 when T8 was above 57 °C and the T-pcm was higher than 19 °C. After that, the IDX-SAHP had two on periods starting at 16:45 and 23:10 respectively when T8 were both lower than 53.0 °C and one off period starting at 18:25 when T8 was above 57 °C. It is noted that the AWHX was always off during this period since the T-pcm was continuously higher than 16.5 °C.

Table 2
System performance for four test days.

Test day	Total power (kW h)	Heating capacity (kW h)	Heating COP
Sunny day with PCM	15.61	77.90	4.99
Cloudy day with PCM	15.83	75.95	4.80
Sunny day without PCM	11.09	52.15	4.70
Cloudy day without PCM	17.11	72.00	4.21

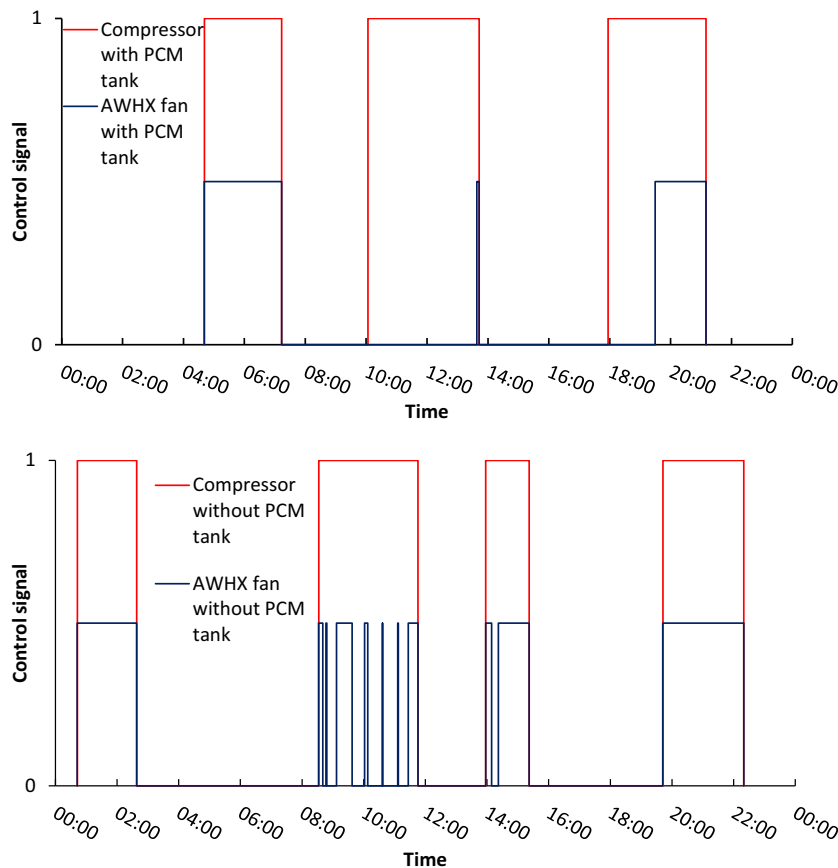


Fig. 15. Variations of compressor and AWHX fan control signals during two cloudy test days.

For the cloudy test day with PCM tank, the same control strategy shown in Fig. 3 would be followed. As shown in Fig. 9, from midnight the system was continued off until at 4:45 am when the water temperature T8 dropped below 53.0 °C. After that, the heat pump compressor had three times running periods and three times off periods due to the variations of T8, as shown in Fig. 15. Meanwhile, there were still two longer and one shorter on periods for the AWHX considering of the corresponding lower solar irradiances and lower T-pcm then. Subsequently, the variations of system power consumption, heating capacity and COP could be found from Figs. 11, 12 and 13 respectively.

For the sunny test day without PCM tank, the system operation on or off was dependent only on the water temperature T8 and any changes of T-pcm shown in Fig. 3 would be ignored. As shown in Fig. 8, from midnight the system was continued off until at 8:00 am when the water temperature T8 dropped below 53.0 °C. After that, the heat pump compressor had four times running periods and four times off periods due to the variations of T8, as shown in Fig. 14. Meanwhile, there were still two longer on periods for the AWHX considering of the corresponding lower solar irradiances then.

Similarly, for the cloudy test day without PCM tank, the system operation on or off was dependent only on the water temperature T8 and any changes of T-pcm shown in Fig. 3 would be ignored. As shown in Fig. 9, from midnight the system was continued off until at 0:45 am when the water temperature T8 dropped below 53.0 °C. After that, the heat pump compressor had four times running periods and four times off periods due to the variations of T8, as shown in Fig. 15. Meanwhile, there were still three longer on and a number of shorter on periods for the AWHX considering of the corresponding lower solar irradiances then.

Respectively, for the cloudy days with and without PCM tank, the variations of system power consumption, heating capacity and COP could be found from Figs. 11, 12 and 13 respectively.

In summary, the total system power consumption, heating capacity and COP are calculated based on measurements for each of these test days and listed in Table 2. It is noted that the heating capacity is the same as the energy input to the WST for each test day. From the measurements, the heating capacities (energy inputs) for three test days were quite similar to each other considering the similar load profiles and feed water temperatures as shown in Figs. 5, 6 and 7. However, the heating capacity (energy input) on the 'Sunny day without PCM' was relatively low considering the higher ambient and feed water temperatures on that day as shown in Fig. 5. From the table, although the total power consumptions and heating capacities varied with different test days, the sunny day with PCM had the maximum COP of 4.99, the COP on cloudy day with PCM the second at 4.80, the COP on sunny day without PCM the third at 4.70 while the COP on cloudy day without PCM the least at 4.21. The test results can demonstrate that the system performance can be significantly improved on various weather conditions if the PCM tank could be integrated.

4. Uncertainty analysis

Taking into consideration the uncertainty of the experiment measurements including the water/glycol mass flow rates, temperatures, power consumptions and pressures, the average uncertainties are calculated for all test days by aid of the Engineering Equation Solver (EES) software (Klein, 2014), which are $\pm 9.32\%$, $\pm 9.28\%$ and $\pm 9.31\%$ for the COP, the heating capacity and the refrigerant mass flow rate, respectively. The uncertainty values are relatively high as the calculations are based on heat balance between the water/glycol and refrigerant sides.

5. Conclusion

A new IDX-SAHP test system has been designed, built and instrumented. There are three operational loops in the system including solar thermal, IDX-SAHP and load profile. A PCM heat exchanger tank was purposely designed and installed in the system solar thermal loop to absorb and store solar energy when applicable and release heat when required. The PCM tank was more compact and efficient comparing to conventional water storage tanks used in IDX-SAHP systems. In addition, an air cooling heat exchanger was selected and also installed between the solar collector and the PCM tank in the solar thermal loop. It was controlled on when ambient air heat source was needed for the IDX-SAHP. A control strategy was intentionally designed and implemented with building management system so as to maintain constant temperature of hot water production and ensure high efficient system operations. Comprehensive measurements were carried out for four test days with different weather conditions (sunny and cloudy) and system structures (with and without PCM tank). The experimental results show that the designed IDX-SAHP system can meet the daily hot water load demand with constant hot water supply irrespective of weather conditions and system structures. In addition, the IDX-SAHP system could have various performance improvements at different weather conditions when PCM tank was integrated. Quantitatively, the average COP of the IDX-SAHP system with PCM tank could increase 6.1% and 14.0% on sunny and cloudy days respectively comparing to those systems without PCM tank integrations. These are based on the weather conditions for different test days illustrated in this paper.

References

- Aguilar, C., White, D.J., Ryan, D.L., 2005. Domestic Water Heating and Water Heater Energy Consumption in Canada. Canadian Building Energy End-Use data and Analysis Centre. CBEEAC 2005-RP-02.
- Ayome, L.M., Duffy, A., McCormack, S.J., Conlon, M., 2011. Validated TRNSYS model for forced circulation solar water heating systems with flat plate and heat pipe evacuated tube collectors. *Appl. Therm. Eng.* 31, 1536–1542.
- Bakirci, K., Yuksel, B., 2011. Experimental thermal performance of a solar source heat-pump system for residential heating in cold climate region. *Appl. Therm. Eng.* 31, 1508–1518.
- Banister, C.J., Wagar, W.R., Collins, M.R., 2014a. Solar-assisted heat pump test apparatus. *Energy Procedia* 48, 489–498.
- Banister, C.J., Wagar, W.R., Collins, M.R., 2014b. Validation of a single tank, multi-mode solar-assisted heat pump TRNSYS model. *Energy Procedia* 48, 499–504.
- Carbonell, D., Haller, M.Y., Frank, E., 2014. Potential benefit of combining heat pumps with solar thermal for heating and domestic hot water preparation. *Energy Procedia* 57, 2656–2665.
- Chen, J., Yu, J., 2017. Theoretical analysis on a new direct expansion solar assisted ejector compression heat pump cycle for water heater. *Sol. Energy* 142, 299–307.
- Deng, S., Dai, Y.J., Wang, R.Z., Matsuura, T., Yasui, Y., 2011. Comparison study on performance of a hybrid solar-assisted CO₂ heat pump. *Appl. Therm. Eng.*, 3696–3705.
- Eicher, S., Hildbrand, C., Bony, J., Bunea, M., Hadorn, J.C., Citherlet, S., 2012. Solar assisted heat pump for domestic hot water production. *Energy Procedia* 30, 571–579.
- Energy Savings Trust, 2008. Measurement of domestic hot water consumption in dwellings. Energy Savings Trust, 1–62.
- Fação, J., Carvalho, M.J., 2014. New test methodologies to analyse direct expansion solar assisted heat pumps for domestic hot water. *Sol. Energy* 100, 66–75.
- Farid, M.M., Khudhair, A.M., Razack, S.A.K., Al-Hallaj, S., 2004. A review on phase change energy storage: materials and applications. *Energy. Convers. Manage.* 45, 1597–1615.
- Freeman, G.A., 1997. Indirect solar-assisted heat pumps for application in the Canada environment (Master thesis). Department of mechanical engineering, Queen's University.
- International Energy Agency, 2007. Energy Use in the New Millennium: Trends in IEA Countries. <<http://www.iea.org/textbase/nppdf/free/2007/millennium.pdf>>.
- Kamel, R.S., Fung, A.S., 2014. Solar systems and their integration with heat pumps: a review. *Energy Build.* 87, 395–412.
- Klein, S.A., 2014. Engineering equation solver (EES) for Microsoft windows operating systems, Professional V9.711-3D, Madison USA, WI: F-Chart software. (available at <<http://www.fChart.com/>> (accessed 31.01.2014).

- Şevik, S., Aktaş, M., Doğan, H., Koçak, S., 2013. Mushroom drying with solar assisted heat pump system. *Energy Convers. Manage.* 72, 171–178.
- Sharif, M.K.A., Al-Abidi, A.A., Mat, S., Sopian, K., Ruslan, M.H., Sulaiman, M.Y., 2015. Review of the application of phase change material for heating and domestic hot water systems. *Renew. Sustain. Energy Rev.* 42, 557–568.
- Sterling, S.J., Collins, M.R., 2012. Feasibility analysis of an indirect heat pump assisted solar domestic hot water system. *Appl. Energy* 93, 11–17.
- Sun, X., Dai, Y., Novakovic, V., Wu, J., Wang, R., 2015. Performance comparison of direct expansion solar-assisted heat pump and conventional air source heat pump for domestic hot water. *Energy Procedia* 70, 394–401.
- Wang, Q., Liu, Y., Liang, G., Li, J., Sun, S., Chen, G., 2011. Development and experimental validation of a novel indirect-expansion solar-assisted multifunctional heat pump. *Energy Build.* 43, 300–304.
- Weiss, W., 2003. *Solar Heated Houses. A Design Handbook for Solar Combisystems IEA SHC Task 26.* James & James Science Publishers, UK.